Analytical Methods

Accepted Manuscript

This article can be cited before page numbers have been issued, to do this please use: C. G. Ambarsari, S. Martinez Jarquin, J. J. R. Koh, G. Needham, K. P. Arkill, V. James, M. W. Taal, J. J. Kim, D. Kim and A. M. Piccinini, *Anal. Methods*, 2026, DOI: 10.1039/D6AY00002A.

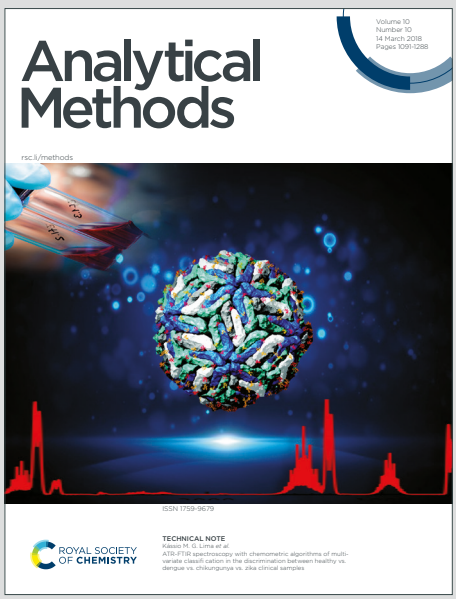

ROYAL SOCIETY OF CHEMISTRY

rsc.li/methods

View Article Online
DOI: 10.1039/D6AY00002A

Optimised Untargeted Metabolomics Workflow for Human Urinary Extracellular Vesicles

Cahyani Gita Ambarsari[1,2,3], Sandra Martinez Jarquin[4], Jasper J. R. Koh[1,5], Grace Needham[1], Kenton P. Arkill[6], Victoria James[7], Maarten W. Taal[2], Jon Jin Kim[8], Dong H. Kim[4,9]*, Anna M Piccinini[1]*

[1]School of Pharmacy, Biodiscovery Institute, University of Nottingham, Nottingham NG7 2RD, UK

[2]Centre for Kidney Research and Innovation, Translational Medical Sciences, School of Medicine, University of Nottingham, Nottingham, UK

[3]Department of Child Health, Faculty of Medicine Universitas Indonesia – Cipto Mangunkusumo Hospital, Central Jakarta, Indonesia 10430

[4]Centre for Analytical Bioscience, Advanced Materials & Healthcare Technologies Division, School of Pharmacy, University of Nottingham, Nottingham NG7 2RD, UK

[5]Department of Pharmacy, National University of Singapore, Singapore 117559, Singapore

[6]School of Medicine, Biodiscovery Institute, University of Nottingham, Nottingham NG7 2RD, UK

[7]School of Veterinary Medicine and Science, Biodiscovery Institute, University of Nottingham, Nottingham NG7 2RD, UK

[8]Department of Paediatric Nephrology, Nottingham University Hospitals, Nottingham, UK

[9]College of Pharmacy, Kyungpook National University, Daegu 41566, Republic of Korea

*Corresponding authors:

Anna Maria Piccinini

e-mail address: anna.piccinini@nottingham.ac.uk

Postal address: Biodiscovery Institute, University of Nottingham, University Park Campus, East Drive, Nottingham NG7 2RD, UK

Dong-Hyun Kim

e-mail address: dong-hyun.kim@nottingham.ac.uk

Postal address: Boots Science Building, University of Nottingham, University Park Campus, East Drive, Nottingham NG7 2RD, UK

View Article Online
DOI: 10.1039/D6AY00002A

Keywords: urinary extracellular vesicles, urinary extracellular vesicle isolation, metabolite extraction, metabolomics, LC-MS, untargeted metabolomics

Abstract

Extracellular vesicles (EVs) have been a key focus in biomarker discovery, with urinary EVs (uEVs), primarily derived from cells of the urogenital tract, providing valuable insights into kidney and urinary tract health and disease. However, progress in uEV-based metabolomics remains limited by variability in EV isolation and extraction approaches. Here, we systematically evaluated and optimised experimental conditions for untargeted metabolite profiling of human uEVs.

We compared three different EV isolation methods, namely precipitation, size-exclusion chromatography, and pH-adjustment with resin separation, and found that precipitation yielded the highest particle count. However, the pH-adjustment with resin separation method produced the highest number of small EVs (30–150 nm), aligning with the primary focus of EV research. Transmission electron microscopy analysis confirmed the presence of well-structured exosomes in these isolates. Moreover, this EV isolation method generated the broadest metabolite coverage.

To identify the most effective metabolite extraction conditions, we compared two established protocols (Liu *et al*. 2023 and Hinzman *et al*. 2022) with an in-house-developed method. Application of the protocol of Liu *et al*. led to the identification of the highest number of metabolites. Considering EV purity, contamination risks and metabolite yield, the combination of the pH-adjustment with resin separation method for uEV isolation with the metabolite extraction protocol of Liu *et al*. was the optimal approach for metabolomics analysis of the uEV cargo.

This study provides an experimentally validated workflow for robust untargeted metabolomics analysis of human uEVs and supports the development of more standardised approaches for EV-based biomarker discovery.

View Article Online
DOI: 10.1039/D6AY00002A

Introduction

Urine is the second most used biofluid for clinical diagnostics after blood owing to its ease of collection in terms of frequency, quantity and non-invasive mode of sampling [1-4]. Under normal physiological conditions, urine contains water, metabolic waste products such as urea and creatinine, salts, ions, a few epithelial cells and extracellular vesicles (EVs)[5]. EVs are lipid-bilayer-encapsulated particles that can be released by all living cells into the extracellular space[6]. EVs are classified by their biogenetic origin and size into exosomes (30–150 nm), which arise from the endosomal pathway[7], microvesicles (100–1,000 nm), which bud from the plasma membrane, migrasomes (500–3,000 nm) and large oncosomes (1–10 μm), which are shed by migrating or cancer cells, respectively[8, 9]; apoptotic bodies (1–5 μm), which form during programmed cell death, and non-vesicular particles like exomeres and supermeres (<50 nm), which have unclear biogenesis[10].

EVs protect and stabilise their molecular cargo, which consists of DNA, mRNA, miRNAs, proteins, lipids and metabolites, in circulation and facilitate cell-to-cell communication. EVs mediate intercellular communication locally and at a distance. They circulate to distant tissues and are taken up by recipient cells via receptor-mediated binding, endocytosis or membrane fusion, delivering their molecular cargo that modulates cell signalling and phenotype[11]. Changes in EV properties or quantity may reflect disease progression or treatment response[12, 13]. Due to their diagnostic potential, EVs have become a major focus in biomarker discovery research over the past decade, with biofluids such as plasma, saliva, cerebrospinal fluid, and urine serving as EV sources[14]. For example, Logozzi *et al*. (2019) analysed exosomes from plasma samples of 80 prostate cancer (PCa) patients and 80 healthy donors and showed that exosomes expressing both CD81 and prostate-specific antigen (PSA) achieved 100% sensitivity and specificity in distinguishing PCa patients from healthy individuals[15]. Similarly, Zhai *et al*. (2018) examined miR-1246 in plasma exosomes as a biomarker for breast cancer, reporting a sensitivity of 100% and a specificity of 92.9% at the optimal cutoff in a study involving 46 breast cancer patients and 28 healthy controls[16]. Additionally, proteins associated with central nervous system (CNS)-derived circulating EVs, including α-synuclein (aSyn) and leucine-rich repeat kinase 2 (LRRK2), have been identified as potential biomarkers for Parkinson's disease[17]. These findings highlight the growing role of EVs in disease detection and monitoring.

View Article Online
DOI: 10.1039/D6AY00002A

Studies about EVs also reported the potential role of urinary EVs (uEVs), which are mainly derived from the epithelial cells lining the urogenital tract and are believed to portray the physiology and pathology of the associated organs[18, 19]. Early research on urogenital tract cancers has paved the way for the development of uEV-based biomarkers for other urogenital tract pathologies such as acute kidney injury, glomerular diseases, and kidney transplantation[1, 13]. In 2019, the FDA granted breakthrough designation to ExoDx™ Prostate IntelliScore (EPI Test, Bio-Techne), an EV-based non-invasive urine test as a home collection kit for prostate cancer diagnostics. By measuring three RNA markers, the use of ExoDx™ has successfully reduced the number of unnecessary prostate biopsies and eliminated the need for digital rectal examination, yet increasing high-grade prostate cancer detection[20-22].

To date, there is no consensus on the optimal EV isolation method in EV research. The balance between EV recovery yield, purity and integrity appears to drive the choice of method among the different available techniques, including ultracentrifugation, density gradient centrifugation, size-exclusion chromatography (SEC), antibody-based affinity capture, ultrafiltration, and polymer-based precipitation[21]. This decision is further influenced by the specific requirements of downstream EV analyses[23, 24]. Similar challenges also arise in studies using uEVs. The isolation of uEVs has been complicated by contamination from non-uEV-associated proteins, such as uromodulin or Tamm-Horsfall glycoprotein[25]. Furthermore, selecting a particular isolation technique can be influenced by the type of urine sample (proteinuric or non-proteinuric) and the downstream analysis employed for "omics" characterisation following the uEV isolation, including genomics, transcriptomics, proteomics, or metabolomics[19].

Standard analytical methods and high-throughput omics technologies have revealed the enormous potential of EV-derived disease biomarkers[1]. In this study, we focus on metabolomics for the analysis of human uEVs. Potential biomarkers can be identified through untargeted metabolomic analysis, which demands effective EV metabolite extraction methods to maximise metabolite release and recovery from the uEVs[26]. This process requires EV membrane permeabilisation followed by metabolite extraction using an organic solvent[27]. The most widely used approach for achieving high metabolite coverage is protein removal via precipitation with cold organic solvents such as methanol, methanol/ethanol, or acetonitrile[28]. Alternative methods include organic solvent mixtures with water such as chloroform-methanol-water or methyl tert-butyl ether[29]. While solid-phase extraction is generally avoided due to its selectivity, it may be useful for volatile organic compounds[27, 30]. Overall, sample preparation should be

View Article Online
DOI: 10.1039/D6AY00002A

non-destructive and non-selective to preserve the wide variety of metabolites while ensuring compatibility with downstream analytical techniques for analysis[27].

Currently, there is no globally recognised standardised protocol for sample preparation from whole urine, uEV isolation, and metabolite extraction[1, 31]. Hence, in this study we sought to optimise the uEV isolation and metabolite extraction steps for an LC-MS-based untargeted metabolomics approach using urine samples from healthy donors. By comparing three different EV isolation approaches (precipitation, SEC, and pH-adjustment with resin separation) and three distinct EV metabolite extraction protocols (Liu 2023, Hinzman 2022, and our in-house developed protocol), we identified the optimal procedures for high-quality yield of uEVs for untargeted metabolomics.

Experimental

Materials

Urine from healthy donors was collected in 100 mL plastic sterile urine containers with a screw cap (Thermo Scientific Sterilin Polystyrene Container, plain label, closure material: polyethylene). cOmplete™, Mini-Protease Inhibitor Cocktail was from Merck Life Sciences, Dorset, UK. LC-MS grade acetonitrile, methanol, and isopropyl alcohol were from Fisher Chemical and used for all steps. Ultrapure water (18.2 MΩ·cm at 25 °C) was dispensed using a SLS Lab Pro PURA-Q+20 R system (SLS, UK) and used for all sample preparations and chromatographic analyses.

Urine sample collection

This study has been reviewed and approved by the School of Pharmacy Research Ethics Committee (Reference number: 009-2019), University of Nottingham. Written informed consent was obtained from healthy donors who provided urine samples. Healthy donors were older than 18 and had no known infection at the time of donation. Random morning urine samples (~200 mL/each) were collected in urine containers and one cOmplete™, Mini-Protease Inhibitor Cocktail tablet was added per ≤50 mL of fresh urine. In addition to irreversible and reversible protease inhibitors, each tabled contains EDTA (3.7 mg per tablet; equivalent to 1 mM EDTA solution in 10 mL).Urine samples were swirled to dissolve the tablet (Fig 1).

View Article Online
DOI: 10.1039/D6AY00002A

Urine sample pre-processing

Urine sample pre-processing was done within 4 hours of sample collection. Urine samples were transferred to Falcon 50 mL conical sterile tubes for centrifugation at 800 x *g* at 4°C for 10 minutes with a swing-bucket rotor (Eppendorf Centrifuge 5810R). The supernatant was aspirated using a serological pipette and transferred to a Falcon 50 mL conical sterile tube and the pellet was discarded. The sample was divided into 15 mL aliquots for uEV isolation and 20 mL aliquots for uEV metabolite extraction (Fig 1). Three replicates were prepared for each protocol, and all samples were stored at -80°C for up to 2 weeks prior to processing.

Optimisation of urinary extracellular vesicle (uEV) isolation

uEVs were isolated using 3 commercially available kits: 1) Total Exosome Isolation Reagent (TEIR; Invitrogen™) - precipitation-based, 2) qEV single/35 nm IZON column – size-exclusion chromatography (SEC)-based, and 3) Urine Exosome Purification Kit (UEPK; Norgen) – pH-adjustment with resin separation-based (Fig 1).

Precipitation-based uEV isolation

15 mL of Invitrogen™ Total Exosome Isolation Reagent (from urine) (Thermo Fisher Scientific, Leicestershire, United Kingdom) was added to 15 mL of urine. The mixture was vortexed until the solution was homogenous. The sample was incubated for 1 hour at room temperature and was then transferred to a clean ultracentrifugation tube (Beckman polycarbonate, catalogue number: 355630) for centrifugation at 10,000 x *g* for 1 hour at 4°C (Sorvall Discovery 100SE Floor Ultra Speed Centrifuge and rotor T-890, Thermo Fisher Scientific, United Kingdom). The supernatant was aspirated and discarded without disturbing the EV-containing pellet, which was resuspended in PBS and vortexed for subsequent analyses[32].

Size-exclusion chromatography (SEC)-based EV isolation

15 mL of urine was concentrated using a Vivaspin® Turbo 15 (100 kDa MWCO PES; product code: VS15T41, Sartorius, Stonehouse, United Kingdom) and centrifugation at 2,000 x *g* at 4°C (Eppendorf Centrifuge 5810R – benchtop centrifuge, swing-bucket rotor, Eppendorf AG, Hamburg, Germany) to a final volume of 150 µL. PBS was degassed by centrifugation at 2,000 x *g* for 10 minutes at room temperature to prevent air bubbles forming in the SEC column's gel bed. qEV single/35 nm – Gen 2 IZON columns and buffer (IZON Science Europe SAS Lyon, France) were equilibrated at room temperature for at least one hour. The top and bottom caps of the column were removed, and the default IZON column buffer was allowed to run through the

View Article Online
DOI: 10.1039/D6AY00002A

column. Next, the column was equilibrated by passing through two column volumes of buffer (a total volume of 6 mL of PBS)[33-35].

Once all the buffer had run through the column, 150 µL of concentrated urine sample was applied to the column with a pipette. The column was topped up with PBS to a total of 550 µL. The first 700 µL of eluate (void volume) from the column were collected using an Eppendorf 1.5 mL safe-lock microtube. Afterwards, the column was loaded with 170 µL of PBS each time. Each 170 µL of eluate, called purified collection volume (PCV), was collected into one Eppendorf 1.5 mL safe-lock microtube. Seven individual fractions of 170 µL were collected and marked as fractions 1, 2, 3, 4, 5, 6, and 7 referring to the PCV sequence. Eluted fractions and void volumes were stored at 4°C for downstream processing and analysis[33-35].

pH-adjustment with resin separation-based EV isolation

1.5 mL of ExoC Buffer from Norgen Urine Exosome Purification Midi kit (Geneflow, Staffordshire, United Kingdom) was added to 15 mL of urine, followed by 600 µL of Slurry E (Norgen). The mixture was vortexed for 10 seconds and incubated for 10 minutes at room temperature. The sample was then vortexed for 10 seconds prior to centrifugation at 800 x *g* for 2 minutes at room temperature (Eppendorf Centrifuge 5810R – benchtop centrifuge, swing-bucket rotor).

The supernatant was removed while the pellet was resuspended in 600 µL ExoR Buffer (Norgen). Afterwards, the sample was vortexed for 10 seconds, followed by incubation at room temperature for 10 minutes, and another 10 seconds of vortexing. Next, it was centrifuged at 50 x *g* at room temperature for 2 minutes. The supernatant was transferred to a mini filter spin column (Norgen). The spin column was centrifuged at 3,500 x *g* for 1 minute at room temperature (Thermo Fresco Scientific 17 Micro Centrifuge, Thermo Fisher Scientific, United Kingdom) to obtain the purified exosome flow through[36].

Nanoparticle tracking analysis of uEVs

Quantitative analysis of the uEVs was done with nanoparticle tracking analysis (NTA) to obtain the uEV concentration and size distribution. ZetaView PMX-220 (Particle Metrix, Germany) was used for the NTA, with parameter settings as described below[37]. Sample dilutions ranged from 1:1 to 1:2500 in PBS to a final volume of 0.6 mL. Dilutions that yielded 100–200 particles per frame value were considered optimal. Default manufacturer's software settings were selected.

View Article Online
DOI: 10.1039/D6AY00002A

EVs were detected using a scientific complementary metal oxide semiconductor (CMOS) camera and a 488 nm laser (blue)[38].

For every measurement, one cycle was performed with 11 cell positions scanned. Moreover, 30 frames per position were captured with the following equipment specific settings: cell temperature of 25°C, autofocus, shutter value of 100, and camera sensitivity of 80. Post-acquisition parameters were set to 5 nm per class on the x-axis to improve data resolution. Only measurements with at least 8 out of 11 valid positions were accepted for subsequent analysis. ZetaView software 8.05.14 SP7 was utilised to analyse the videos using minimal area 10, maximal area 1000, and minimal brightness 30. Data analyses include the size [mean, peak, and range (nm)] and concentration (particles/mL)[39].

Western blotting analysis

Western blotting was performed to assess the presence of CD9 and Annexin V and the absence of GM130 in isolated uEVs. uEV preparations were lysed in 10X Laemmli sample buffer supplemented with 5% (v/v) β-mercaptoethanol. Lysates were then sonicated for 10 seconds and boiled at 95°C for 5-10 minutes before being placed on ice for 15 minutes. Samples were then centrifuged at 16,200 × g for 10 minutes at 4°C to remove insoluble debris. Supernatant (20–30 µL) was then collected and loaded into a 12% polyacrylamide gel. SDS-PAGE was run at 15 mA until proteins migrated through the stacking gel, followed by 20-25 mA for separation.

View Article Online
DOI: 10.1039/D6AY00002A

Proteins were wet transferred to nitrocellulose membranes using 1X Transfer Buffer containing 20% (v/v) methanol at 4°C (350 mA, 50 minutes). Membranes were blocked in 5% (w/v) bovine serum albumin (BSA) in tris-buffered saline (TBS) containing 0.1% Tween 20 (TBST) for 1 hour at room temperature, then incubated overnight at 4°C with primary antibodies against human CD9 (#13174), Annexin V (#8555), and GM130 (#12480, Cell Signalling Technology, Leiden, Netherlands). Antibodies were diluted 1:1000 in 5% BSA in TBST. Membranes were washed three times (10 minutes each) in TBST and incubated with anti-rabbit HRP-conjugated secondary antibodies (Dako, P0217, 1:5000) diluted in 5% milk/TBST for 1 h at room temperature. After three additional washes in TBST, bands were detected using enhanced chemiluminescence (Amersham™ ECL Western Blotting Detection Reagent, Cytiva, Buckinghamshire, UK) and visualised using a LAS-4000 (FujiFilm). Where required, membranes were stripped using 1X RE-BLOT PLUS (Millipore) solution and re-probed as described above.Transmission electron microscopy of uEVs

The morphological characterization of uEVs was done using a transmission electron microscope (TEM). Standard carbon-coated mesh grids (C200Cu, EMResolutions) were used for TEM imaging. In order to adsorb sufficient uEVs, glow-discharged copper grids were floated on a suspension of uEVs fixed with 3% glutaraldehyde in cacodylate buffer. All samples were then negatively stained with 1% aqueous uranyl acetate (0.2 µm filtered) and examined with FEI Tecnai G2 12 Biotwin (Thermo Fisher Scientific, United Kingdom), 100 kV at nominal magnifications typically ranging from 2,900× to 49,000×.

Optimisation of uEV metabolite extraction

Metabolites were extracted from isolates obtained with the SEC-based uEV isolation method. Prior to extraction, uEV isolates were freeze-dried with a Thermo Scientific Heto PowerDry PL3000 Freeze Dryer (Thermo Fisher Scientific, United Kingdom). The weight of the dried uEV isolates was measured to allow for sample normalisation by the addition of an appropriate volume of solvent used in each of the metabolite extraction protocols described below (Fig 2).

Liu et al. (2023)-based metabolite extraction

Freeze-dried uEVs were resuspended in 50 µL of PBS. The suspension was then combined with 950 µL of extraction solution composed of methanol:acetonitrile:water (2:2:1). After three freeze-thaw cycles using liquid nitrogen, each sample was vortexed for 30 seconds, followed by 10 minutes of sonication (Ultrawave ultrasonic bath, Cardiff, United Kingdom) with the sonication bath filled with ice and water to prevent overheating. The samples were then incubated at 40°C for an hour (Fisher Scientific DMU12 12 L Water Bath Lab, Loughborough, United Kingdom),

View Article Online
DOI: 10.1039/D6AY00002A

followed by centrifugation at 13,500 x *g* at 4°C for 15 minutes. Subsequently, 1000 µL of the supernatant was dried using a vacuum concentrator (Jouan centrifugal evaporator, RC10.22, United Kingdom). The dried pellet was then resuspended in 200 µL of extraction solution (methanol:acetonitrile:water, 2:2:1). After 30 seconds of vortexing and 10 minutes of sonication, the samples were centrifuged at 13,500 x *g* at 4°C for 15 minutes. Finally, the supernatant was transferred to an LC-MS amber vial (Waters LCGC, 2 mL amber glass vial, blue polypropylene screw cap with polytetrafluoroethylene (PTFE)/silicone septa) for subsequent LC-MS analysis[40].

Hinzman et al. (2022)-based metabolite extraction

Dried uEV samples were resuspended in 50 µL of PBS and were subjected to heat shock through three cycles of incubation in dry ice for 30 seconds, followed by incubation in a 37°C water bath for 90 seconds per cycle. After one minute of sonication, samples were incubated on ice for 20 minutes. Next, 75 µL of extraction solution (isopropyl alcohol:methanol:water, 4:2.5:3.5), pre-chilled to 4°C, were added. Subsequently, samples were vortexed and kept on ice for 20 minutes. Following the addition of 75 µL of acetonitrile pre-chilled to 4°C, the samples were vortexed for 30 seconds and incubated at 4°C for 20 minutes. Finally, samples were centrifuged at 13,000 x *g* for 20 minutes at 4°C, and the resulting supernatants were then transferred to MS amber vials for MS analysis[41].

In-house developed and optimised metabolite extraction protocol

Dried uEVs were resuspended in 200 µL of methanol and vortexed for 30 seconds. Samples underwent five freeze-thaw cycles, using liquid nitrogen for 10–20 seconds followed by thawing on ice to ensure complete defrosting and enhance metabolite extraction from uEVs. Samples were vortexed for 30 seconds between each cycle. After centrifugation at 13,000 x *g* for 20 minutes at 4°C, 100 µL of supernatant was transferred to an LC-MS amber vial for subsequent LC-MS analysis.

Untargeted metabolomics

For untargeted metabolomics analysis, the solutions obtained using the three metabolite extraction protocols (Liu, Hinzman, and in-house) were collected in triplicate. 20 µL of each sample was mixed to prepare the quality control (QC) sample for checking instrument performance.

View Article Online
DOI: 10.1039/D6AY00002A

LC-MS analysis was performed using a Q-Exactive Plus mass spectrometer (MS) equipped with Dionex U3000 UHPLC system (Thermo Fisher Scientific, Hemel Hempstead, UK). Metabolites in the samples (10 µL, 4 °C) were separated on a ZIC-pHILIC column (4.6 × 150 mm, 5 µm particle size, Merck Life Science UK Limited, Dorset, UK). The column was maintained at a flow rate of 300 µL/minute and temperature of 45°C for 24 minutes. The gradient started with 20% mobile phase A (20 mM ammonium carbonate in water) and 80% of mobile phase B (acetonitrile) and increased to 95% A over 15 minutes, then the composition was returned to its initial conditions in 2 minutes and the column was re-equilibrated for 7 minutes. The MS was operated in ESI+ and ESI− switching acquisition modes for LC-MS profiling of the samples. For MS parameters, spray voltage was 4.5 kV (ESI+) and 3.5 (ESI−), and capillary voltage was 20 V (ESI+) and −15 V (ESI−). The sheath, auxiliary and sweep gas flow rates were 40, 5 and 1 (arbitrary unit), respectively, for both modes. Capillary and heater temperatures were maintained at 275 and 150 °C, respectively. The mass spectrometer was operated in full-MS/dd-MS2 mode. MS1 spectra were acquired in a scan range of m/z 70–1050. The resolution was set to 70,000 at m/z 200, and the automatic gain control (AGC) target was set to 3×10^6 with a maximum ion injection time of 100 ms. Data-dependent MS/MS spectra were acquired at a resolution of 17,500 at m/z 200.

Data processing, including metabolite identification, was performed by Compound Discoverer 3.3 (Thermo Fisher Scientific, Hemel Hempstead, UK) using a tailored untargeted metabolomics workflow. Metabolite identification was performed by matching accurate masses of the detected peaks with metabolites in BioCyc (human), the Human Metabolome Database and KEGG. Identification levels reported are according to the metabolomics standards initiative [40, 41]: level 1, match of accurate mass, MS/MS fragmentation and retention time to an authentic standard; level 2, match of accurate mass and retention time (two orthogonal data) to the authentic standard or match of accurate mass and MS/MS spectrum with compound in spectral databases; level 3, match of accurate mass and predicted retention times or predicted MS/MS spectra or both due to the lack of standards; level 4, unambiguously assigned molecular formulas where insufficient evidence exists to propose possible structures.

We normalised all uEV isolates by dry weight, adding a proportional amount of the solvent depending on the extraction protocol.

View Article Online
DOI: 10.1039/D6AY00002A

Statistical analysis

For the untargeted metabolomics data, univariate analysis was performed by Compound Discoverer after log10 transformation (t-test with Benjamini–Hochberg false-discovery rate correction) and multivariate analysis (MVA) by Simca P+16 (Umetrics AB, Umea, Sweden), with imported datasets mean-centred and Pareto-scaled for MVA. The permutation test was performed with 200 permutations.

Unless otherwise stated, the data presented in text and figures represent the mean ± standard error of the mean (mean ± SEM). One-way analysis of variance (ANOVA) followed by Tukey's multiple comparison test was used to compare the mean of each group with the mean of every other group. Two-way ANOVA followed by Sidak's post hoc test was used to compare data grouped by two factors. Statistical analyses were performed using GraphPad Prism (version 10.3.1). Statistical significance was expressed as follows: * $p < 0.05$, ** $p < 0.01$, *** $p < 0.001$, **** $p < 0.0001$, and p-value > 0.05 were classified as not significant.

Results and discussion

Comparison of uEV isolation methods

In this study, we compared three uEV isolation methods: precipitation-based (TEIR; Invitrogen™), SEC (IZON), and pH-adjustment with resin separation (Norgen). This comparative analysis evaluated yield, size distribution and morphology of the isolated uEVs. Prior to this, the presence of EVs and the absence of contaminating particles was assessed by Western blotting analysis of the uEV isolates. Detection of positive EV markers CD9, a tetraspanin, and Annexin V, a protein that associates with phosphatidylserine on the outer leaflet of the EV-membrane, confirmed the presence of EVs. The absence of the negative marker GM130, which indicates contamination from the Golgi apparatus, informed the purity of the different uEV isolates (Fig. 3a).

Particle concentration and size distribution

To measure particle concentration and size distribution of the uEVs obtained with the three different isolation approaches, we performed NTA. The precipitation-based uEV isolation method yielded the highest particle concentration $(3.06\pm2.29)\times10^{11}$ particles/mL, followed by SEC $(1.45\pm1.28)\times10^{11}$ particles/mL, whereas the pH-adjustment with resin separation-based method yielded the lowest $(3.88\pm2.52)\times10^{9}$ particles/mL (Fig. 3b). As shown in Figure 3c, the size distribution of uEVs varied depending on the isolation method used. uEVs isolated by pH-adjustment with resin separation included a higher proportion of smaller uEVs [peak at 105 nm,

View Article Online
DOI: 10.1039/D6AY00002A

($5.7\pm0.05)\times10^6$ particles/mL; range: 15–485 nm] than the precipitation-based method [peak at 115 nm, ($4.8\pm0.4)\times10^6$; range 15-515 nm] and SEC [peak at 125 nm, ($3.7\pm0.7)\times10^6$; range: 15–555 nm].

The higher total particle concentration and the broader size distribution peak observed with the precipitation-based method could reflect its ability to isolate EVs across a broader range of sizes. However, the method allows for co-precipitation of contaminants, including proteins and non-EV-associated extracellular nucleic acids, which can compromise the purity of the isolated EVs[42]. A similar trend was observed in a study by Reseco *et al*. (2024), which analysed saliva samples and found that precipitation-based isolation resulted in the highest EV concentration and broader size distribution compared to other EV isolation methods, including pH-adjustment with resin separation, SEC, and ultracentrifugation[43]. Precipitation-based isolation relies solely on the physical process of precipitation, without additional conditioning steps such as chemical modifications or pH adjustments that can enhance isolation efficiency and purity. This makes it a straightforward and user-friendly technique. However, precipitation methods are prone to polymer contamination, often requiring extensive pre- and post-clean-up steps[44]. In our study, the precipitation-based method using TEIR requires ultracentrifugation, which can potentially result in EV damage. Furthermore, ultracentrifugation can result in the co-isolation of non-EV particles and aggregates[45].

Similar to a previous report[43], our study found that the number of particles isolated using SEC is higher than that obtained using the pH-adjustment with resin separation method. This could be explained by the intrinsic ability of SEC to separate particles based on their physical properties (i.e. size and shape) and thus recover a large number of particles[46]. However, this method may result in the co-isolation of larger vesicles or non-EV particles, reducing its specificity for exosome isolation. Although SEC does not create an absolute dichotomy between components such as lipids, exosomes, and apoptotic bodies, it remains an effective method for size-based separation[47]. Some SEC-based products, including qEV35 and qEV70 separation columns, have been favoured for their high-purity isolates, the intact structure of isolated exosomes, and good reproducibility. Despite its advantages, SEC is considered time-consuming[44]. While SEC effectively recovers many particles, our study found that it yields a peak size of 125 nm with a broad size distribution (15–555 nm), capturing EVs larger than exosomes. The presence of these larger EVs reduces the specificity of SEC for exosome isolation and increases the risk of contamination with unwanted particles, which can confound downstream analyses[48]. Although

View Article Online
DOI: 10.1039/D6AY00002A

SEC is useful for isolating a wide range of EVs, it may not be ideal for studies requiring high specificity in targeting small EVs. Additionally, SEC-based EV isolation from protein-rich biofluids, particularly blood plasma, is prone to co-isolation of soluble proteins (e.g. immunoglobulins and Ig-based therapeutics) due to the high abundance of albumin, which can result in protein saturation of the SEC column [49].

The pH-adjustment with resin separation-based EV isolation method has been shown to efficiently isolate smaller EVs (30–50 nm), which aligns with our findings. It isolates EVs by means of a Silicon Carbide (SiC) resin, which selectively binds exosomes in biofluid samples[43], yielding EV fractions with higher purity, lower protein contamination and higher levels of exosomal marker proteins and RNA content, making this method well-suited for downstream analyses such as RNA-seq[50]. Additionally, this method produces the purest isolates in terms of lipoprotein contamination, compared to SEC and precipitation-based methods, which often yield samples with detectable levels of ApoB[51].Based on our work in this study, we acknowledge that, compared to the other two EV isolation methods, a key advantage of the pH-adjustment with resin separation-based method is its practicality. Because it does not require specialised equipment, it is more cost-effective and better suited for implementation and translation into routine clinical practice in line with the World Health Organization's criteria for point-of-care tests highlighting that effective diagnostic tools should be affordable, user-friendly, rapid, robust, and deliverable with minimal instrumentation, especially when they are to be deployed outside highly specialised laboratory settings [52-55]. A potential limitation of the pH-adjustment with resin separation isolation method is the relatively low yield of EVs, compared to precipitation-based and SEC methods, particularly when working with diluted biofluids such as urine[50].

EV morphology

Negative staining TEM was used to analyze the morphological characteristics of the uEVs that we isolated with the three distinct methods. uEVs obtained with both the precipitation-based method and SEC were clearly identifiable and their structure, which displayed the characteristic lipid bilayer membrane, was easily visualized with minimal background interference (Fig. 3b-c). Analysis also confirmed that the vesicles contained in these isolates were heterogenous in size, as measured by NTA (Fig. 3c), and shape (Fig. 3d-e). TEM analysis of the uEVs isolated with the pH adjustment and resin separation-based method revealed the presence of smaller vesicles (Fig. 3h-i), in agreement with the NTA measurements (Fig. 3c), with spherical morphology. Despite a higher background noise, which could be attributed to residual reagent interference,

View Article Online
DOI: 10.1039/D6AY00002A

the structure of the vesicles clearly indicated the presence of a lipid bilayer (Fig. 3h-i). Together, these data confirm uEV presence in all isolates and smaller-size vesicles in isolates obtained using the pH adjustment and resin separation-based method.

Metabolomic profiling of EVs

uEV isolation for untargeted metabolomics analysis

In order to identify which of the three EV isolation methods evaluated in this study provides optimal metabolite-containing uEV-rich isolates for untargeted metabolomics analysis, we subjected uEVs to metabolite extraction using our in-house protocol (Fig 2). uEVs isolated using the pH-adjustment with resin separation-based method had a significantly higher number of mass ions (4,411) compared to precipitation-based (2,879) and SEC (167) (Table 1). Reagent blank samples were processed alongside all samples for each EV isolation method. Blank samples were used as the baseline for statistical filtering to remove non-specific signals. Only features with adjusted p-value <0.05, Log_2Fold Change >2, and putative annotation based on accurate mass and isotopic fit (in silico-predicted composition) for uEV isolates versus blanks, were retained for further analysis. After applying these three criteria and removing duplicate peaks based on the chromatogram, the number of significant putatively identified metabolites was higher for pH-adjustment with resin separation-based (204 metabolites), followed by precipitation-based (153 metabolites) methods (Figure 4a). In the case of uEVs isolated using SEC, no metabolites met the criteria (Table 1). Metabolites were annotated based on accurate m/z and isotopic fit using in silico formula prediction (Predicted Compositions). No MS/MS spectral matching or authentic standards were used; thus, identifications are reported at Metabolomics Standards Initiative (MSI) Level III[56]. These findings suggest that, compared to the SEC EV isolation method, the precipitation-based and pH-adjustment with resin separation-based methods yielded higher numbers of putatively identified metabolites, making it the preferred approach for comprehensive metabolic profiling, particularly in exosome-derived metabolomics.

Figure 4a highlights the number of unique and common metabolites that were extracted from uEVs isolated using either the precipitation-based method or the pH-adjustment with resin separation-based method, illustrating key differences in metabolite profiles amongst the two uEV isolation techniques. A qualitative comparison of metabolite classes revealed clear differences between the two viable isolation methods. Both methods yielded metabolites belonging to diverse chemical classes, including benzenoids, C/S/N-containing organic compounds, lipids,

View Article Online
DOI: 10.1039/D6AY00002A

nucleosides, nucleotides, organic acids, organoheterocyclic compounds, phenylpropanoids, and polyketides (Fig 4b). However, uEVs isolated by precipitation contained fewer metabolites across most classes with particularly poor detection of lipids, aromatic compounds, heterocyclic compounds, and nucleotide-related metabolites. In contrast, the pH-adjustment/resin method consistently produced broader chemical coverage and recovered a more comprehensive set of metabolites characteristic of small EV cargo. In line with this, metabolic pathway analysis returned commonalities and differences between the two types of uEV isolates. On the one hand, arginine biosynthesis, alanine, aspartate and glutamate metabolism and histidine metabolism pathways were represented in both types of uEV isolates. On the other hand, lysine degradation, ascorbate and aldarate metabolism pathways were unique to uEVs obtained by precipitation, whereas taurine and hypotaurine metabolism and cysteine and methionine metabolism pathways were enriched only in uEVs isolated via the pH-adjustment with resin separation-based method (Fig. c-e). Together, these results demonstrate that uEVs obtained through different isolation techniques differ not only in quantity and size, but also in their metabolic cargo. These results also identify the pH-adjustment with resin separation-based method as the optimal uEV isolation approach for downstream metabolomics analysis, compared to the precipitation-based and SEC uEV isolation methods.

uEV metabolite extraction

Having identified the pH-adjustment with resin separation method as the optimal uEV isolation method for untargeted metabolomics, we next sought to establish a suitable uEV metabolite extraction protocol. This is particularly important given the small size of EVs and, consequently, the low abundance of cargo. For this, we compared three different extraction protocols, two previously reported (Liu *et al.* 2023 and Hinzman *et al*. 2022) and an in-house developed protocol. Figure 2 provides an illustration and side-by-side comparison of the specific methods and conditions used in each protocol. The total number of mass ions identified by LC-MS following metabolite extraction using the Liu, Hinzman, and in-house protocols were 2,118, 1,561, and 1,162, respectively. Blanks were processed alongside all samples for each metabolite extraction method. These blanks were used as the baseline for statistical filtering to remove non-specific signals. Only features with Log_2Fold Change >2 and putative annotation based on accurate mass and isotopic fit (in silico-predicted composition) for uEV metabolites of each extraction protocol, compared to blanks, were retained for further analysis. After applying these two criteria and removing duplicate peaks based on the chromatogram, the number of significant metabolites was 195 (Liu), 147 (Hinzman), and 138 (in-house) (Table 2). Metabolites were annotated based on

View Article Online
DOI: 10.1039/D6AY00002A

accurate m/z and isotopic fit using in silico formula prediction. No MS/MS spectral matching or authentic standards were used; thus, identifications are reported at Metabolomics Standards Initiative (MSI) Level III[56]. Despite variations in the number of detected metabolites, 71 metabolites were common to all three protocols with further 33 metabolites shared between Liu and Hinzman protocols, 28 between Liu and in-house protocols and 13 between Hinzman and in-house protocols (Fig. 5a). Globally, the Liu extraction protocol allowed the identification of the highest number of metabolites (Fig. 5a).

The identified metabolites spanned diverse chemical classes, including benzenoids, C/S/N-containing organic compounds, lipids and lipid-like molecules, nucleosides, nucleotides and analogues, organic acids and derivatives, and organoheterocyclic compounds (Fig. 5b). Pathway analysis revealed the significant metabolic processes carried out by the coordinated function of the identified metabolites, with those extracted using the protocol of Liu being enriched in the highest number and type of pathways (Fig. 5c-f). Together, these comparative analyses demonstrate that the combination of chemical and physical methods in the protocol of Liu is the most effective in extracting metabolites from uEVs.

Liu *et al*.'s extraction protocol yielded a higher number of detected metabolites, which may be attributable to its more aggressive EV lysis and extraction workflow compared with that of Hinzman *et al*. and our in-house protocol[57, 58]. In particular, the combination of repeated sonication, a 1-hour incubation at 40°C following sonication, and the use of an acetonitrile:methanol:water mixture, 2:2:1 for metabolite extraction, is likely to enhance disruption of EV membranes and release of intraluminal metabolites. Compared with a more standard cold organic extraction without prolonged heating, this approach may also improve recovery of certain lipids and membrane-associated small molecules and modestly increase solubilisation of more polar metabolites due to the aqueous fraction[59, 60].

Reproducibility remains a major challenge in the application of metabolomics-based methods to disease biomarker discovery involving EVs as the source of metabolites. This is influenced not only by the difficulty in obtaining sufficiently large patient/donor cohorts, and diversity in ethnicity, gender, and geographical region, but also methodological variability across studies. As demonstrated in the present study, differences in uEV isolation, metabolite extraction, and data normalisation protocols can substantially influence the metabolite detected.

View Article Online
DOI: 10.1039/D6AY00002A

A representative example is the study by Puhka *et al*. (2017), who analysed uEVs from healthy donors (n=3) using ultra-performance liquid chromatography-tandem mass spectrometer (UHPLC-MS-MS) and relatively large urine volumes (38-52 mL)[61]. Their workflow involved differential centrifugation for uEV isolation, and metabolite extraction using ACN:H_2O (80:20) with 1% FA) combined with repeated vortexing and sonication[61]. The resulting metabolite profile differed markedly from ours, with 10 most abundant metabolites including creatinine, L-cystathionine, gamma-glutamylcysteine, guanidinoacetic acid, 4-hydroxyproline, kynurenic acid, glucoronate, pantothenic acid, 4-pyridoxic acid, and 1-methylhistamine[61]. In contrast, despite starting with a urine volume of 20 mL, our study obtained a higher concentration of uEVs whereas Puhka *et al*. reported 1.9 x 10^{10} particles/mL from 38–53 mL of urine following differential centrifugation[61]. These differences in uEV yield reflect key methodological distinctions between isolation procedures.

Puhka *et al*. later applied a targeted metabolomics method to prostate cancer samples, detecting a range of 42–51 metabolites out of 102 targeted compounds in prostate cancer patients after prostatectomy[61]. Using an untargeted approach, our study identified only 167 metabolites from uEV isolated with SEC[41], further illustrating how methodological variation, particularly in EV isolation, shapes metabolite coverage. Together, these examples showing inconsistencies highlight the urgent need for standardised workflows in uEV isolation and metabolomics to improve the reliability, comparability, and reproducibility of biomarker discovery studies [62].

In addition to differences in uEV isolation procedures, the methods used for metabolite extraction must also be considered when evaluating variability across studies. Sonication, included in Liu and Hinzman protocols, disrupts the integrity of vesicular membranes through high frequency cavitation, thereby enhancing the release of metabolites that would otherwise remain encapsulated[63]. While this can improve metabolite recovery, cryo-TEM studies confirm that sonication can deform vesicles and puncture membrane[64], and it may also reduce translocation of positively charged lipids to the outer membrane causing vesicle aggregation. Such aggregated structures can hinder solvent accessibility and, in turn, compromise extraction efficiency and metabolomic coverage[65].

Freeze-thaw cycling, which is incorporated into all three extraction protocols in our study, provides an alternative mechanism of membrane disruption, enabling the release of their internal contents, including metabolites, into the surrounding environment through repeated freezing and

View Article Online
DOI: 10.1039/D6AY00002A

thawing[40]. Organic solvents represent another widely used strategy for metabolite extraction as they destabilise the lipid bilayer of EVs and solubilise a broad range of metabolites. Methanol and acetonitrile frequently employed with Liu's extraction protocol using a combination of methanol and acetonitrile, Hinzman's protocol using methanol and isopropyl alcohol. Our in-house protocol, on the other hand, used methanol alone. Despite these methodological differences, all protocols rely on polar solvents, which effectively extract the molecular cargo from EVs[66]. Polar solvents allow EV metabolite extraction as they effectively disrupt the EV lipid bilayer owing to their ability to interact with the EV membrane-associated lipids, which possess a polar head with a phosphate group and other polar and hydrophilic chemical groups that face outwards, being attracted to water[67, 68]. Specifically, methanol disrupts the electrostatic interactions and hydrogen bonding networks between proteins and lipids[69]. However, despite being widely used, methanol can introduce solvent-drived artefacts during the sample extraction process, complicating metabolomics research, emphasising the need for careful optimisation[70]. Finally, acetonitrile, another commonly used solvent, has been shown to destabilise EV membranes significantly. A study by Yoshida *et al*. (2018) demonstrated that the addition of acetonitrile leads to the deformation of vesicles, including the bending of the lipid bilayer and, in some cases, vesicular bursting[71]. This destabilization effect increases with the acetonitrile concentration, with concentrations above 20% inducing spontaneous curvature and eventual rupture of the vesicle. Consequently, the selection of solvent or solvent combinations and ratios, should be tailored to the chemical properties of the metabolites of interest and the desired balance between extraction strength and EV membrane disruption.

To evaluate the reproducibility of our methodological workflow, we performed independent experiments utilising urine from different donors (n = 3; biological replicates). Particle concentration (4.63×10^9 - 6.30×10^9 particles/mL), number of mass ions (1167 – 1740) and metabolite categories were consistent across biological replicates (data not shown), indicating that both uEV isolation by pH-adjustment with resin separation and metabolite extraction using the Liu protocol followed by LC-MS analysis produce reproducible results across biological replicates, supporting the robustness of the proposed methodological workflow for downstream metabolomics applications.”

View Article Online
DOI: 10.1039/D6AY00002A

Conclusion

This work has established an optimized workflow for untargeted metabolic profiling of human urinary EVs. Through a systematic comparison of three different uEV isolation methods and three metabolite extraction protocols from uEVs, we demonstrated that pH-adjustment with resin separation provides superior recovery of intact, small EVs with broader metabolite yields than precipitation- and SEC-based methods. Furthermore, we found that a metabolite extraction protocol, combining a methanol:acetonitrile:water, 2:2:1 solvent system with freeze-thaw cycles, vortexing, and sonication, effectively extracts metabolites from uEVs. Integration of the two methodological approaches provides a robust workflow for comprehensive characterisation of the metabolome of uEVs, thereby supporting the identification of disease biomarkers and the discovery of new therapeutic targets.

View Article Online
DOI: 10.1039/D6AY00002A

List of tables

Table 1. Mass ion yield across different uEV isolation methods.

uEV Isolation Method	Number of Mass Ions or Metabolites	
	All Mass Ions	Putatively Identified Metabolites*
Precipitation	2879	153
SEC	167	0
pH-adjustment with resin separation	4411	204

*Selection criteria: adjusted p-value <0.05, $\log_2$ fold change >2, and putative annotation based on accurate mass and isotopic fit (in silico-predicted composition) for uEV isolates versus blanks. Duplicate peaks were removed based on chromatogram.
uEV: urinary extracellular vesicles; SEC: size exclusion chromatography.

Table 2. Mass ion yield across different uEV metabolite extraction methods.

Metabolite Extraction Method	Number of Mass Ions or Metabolites	
	All Mass Ions	Putatively Identified Metabolites*
Liu *et al*. (2023)	2118	195
Hinzman *et al*. (2022)	1561	147
In-house protocol	1162	138

*Selection criteria: adjusted p-value <0.05, $\log_2$ fold change >2, and putative annotation based on accurate mass and isotopic fit (in silico-predicted composition) for uEV isolates versus blanks. Duplicate peaks were removed based on chromatogram.
uEV: urinary extracellular vesicles.

View Article Online
DOI: 10.1039/D6AY00002A

Figures

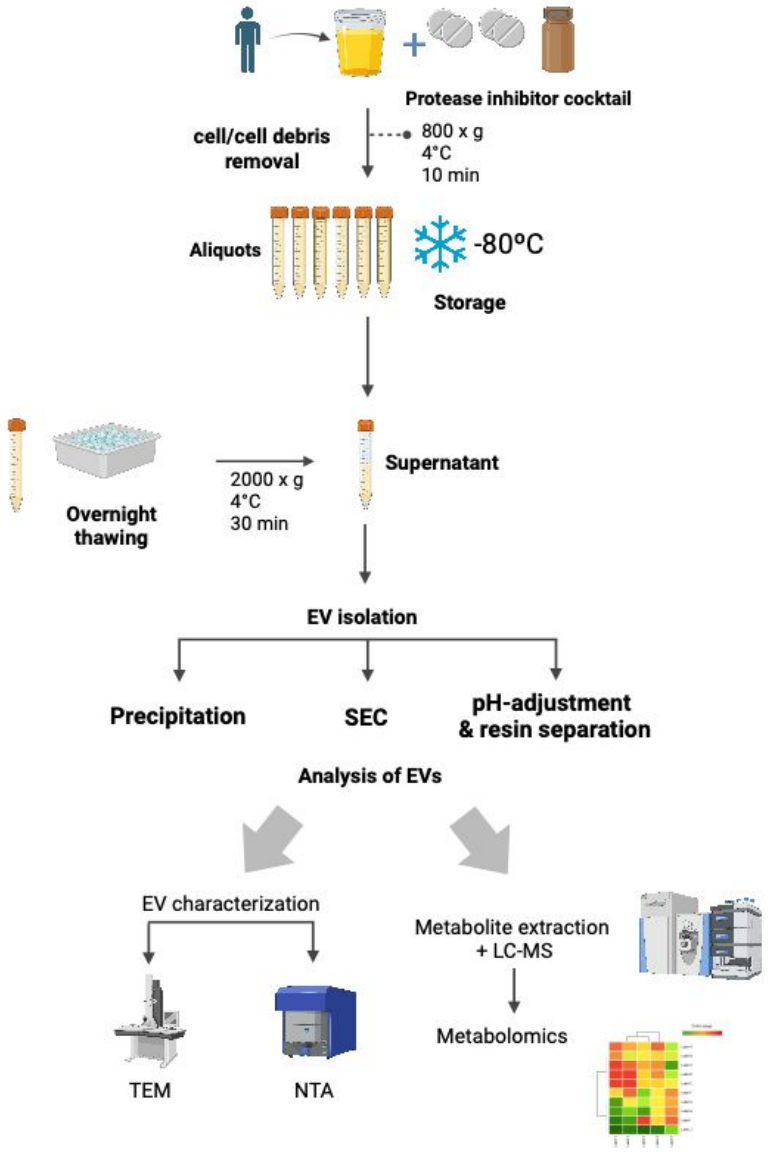

Fig 1. Workflow of the methodological approach. Urine samples containing extracellular vesicles (EVs) were treated with a protease inhibitor cocktail, cleared of debris by sequential centrifugation, and stored at -80°C. Upon thawing, EVs were isolated using precipitation , size-exclusion chromatography (SEC), or pH-adjustment with resin separation-based methods. The isolated EVs were characterized by electron microscopy and nanoparticle tracking analysis and subjected to metabolomic profiling. Abbreviations: EV: extracellular vesicle; LC-MS: Liquid

View Article Online
DOI: 10.1039/D6AY00002A

chromatography–mass spectrometry; NTA: nanoparticle tracking analysis; SEC: size-exclusion chromatography; TEM: transmission electron microscopy. Created with https://BioRender.com.

Created in BioRender. Ambarsari, C. (2025)
https://BioRender.com/zv0rc2n

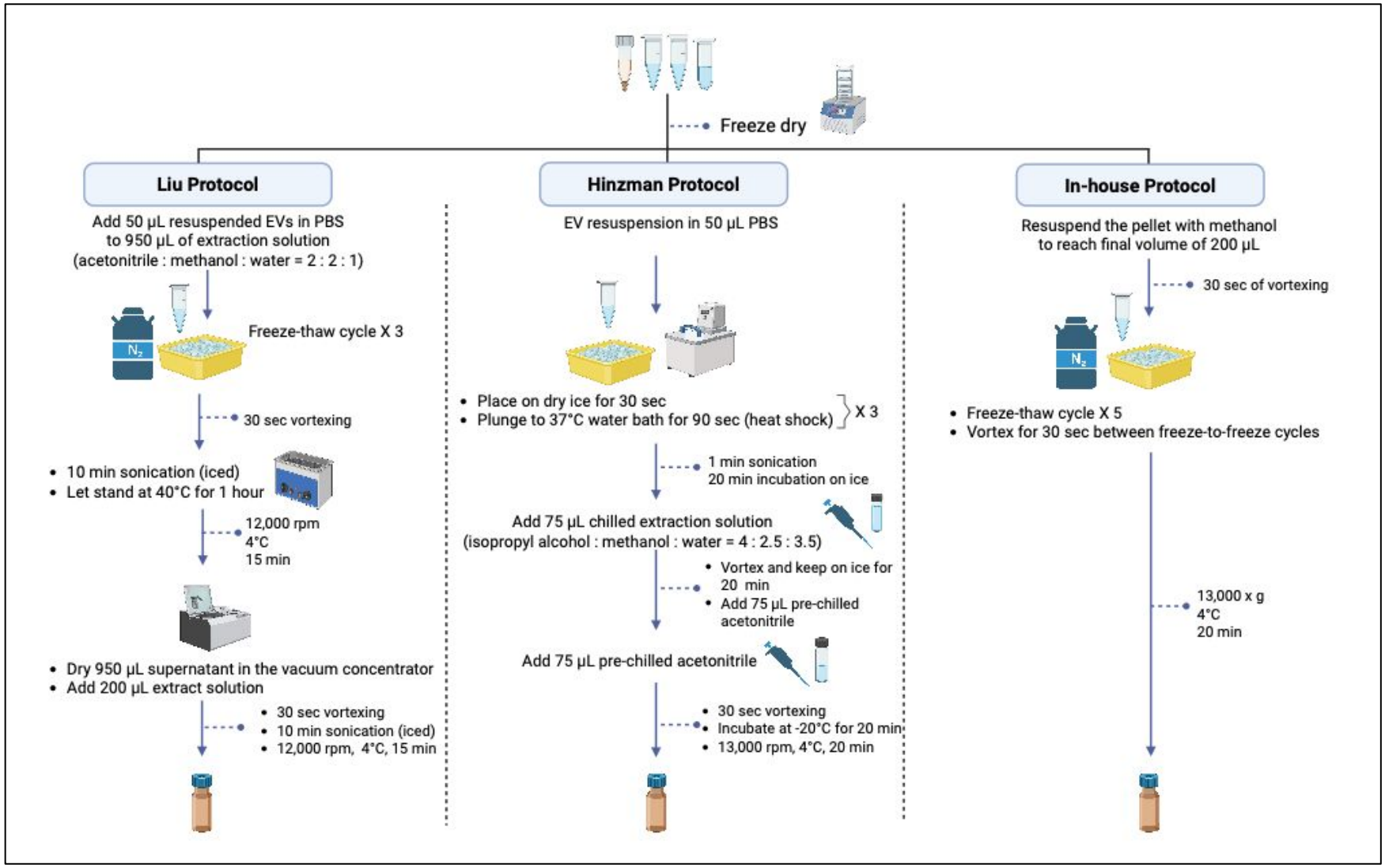

Fig 2. Workflow of metabolite extraction methods. 1) In the protocol of Liu (left), the dried uEVs were resuspended in PBS, mixed with extraction solution, freeze–thawed, vortexed, sonicated, incubated at 40°C, and centrifuged. After drying, extraction solution was

re-added, followed by vortexing, sonication, and centrifugation. 2) In the protocol of Hinzman (middle), dried EVs were resuspended in PBS, heat-shocked (dry ice/37°C), sonicated, and chilled. Extraction buffer and acetonitrile were added with vortexing and incubation on ice and at –20°C. 3) In in-house protocol (right), dried EVs were resuspended in methanol, vortexed, and subjected to five freeze–thaw cycles with intermittent vortexing, followed by centrifugation. *methanol:acetonitrile:water, 2:2:1 †isopropyl alcohol:methanol:water, 4:2.5:3.5. Created with https://BioRender.com.

Created in BioRender. Ambarsari, C. (2025)
https://BioRender.com/zffm3qh

View Article Online
DOI: 10.1039/D6AY00002A

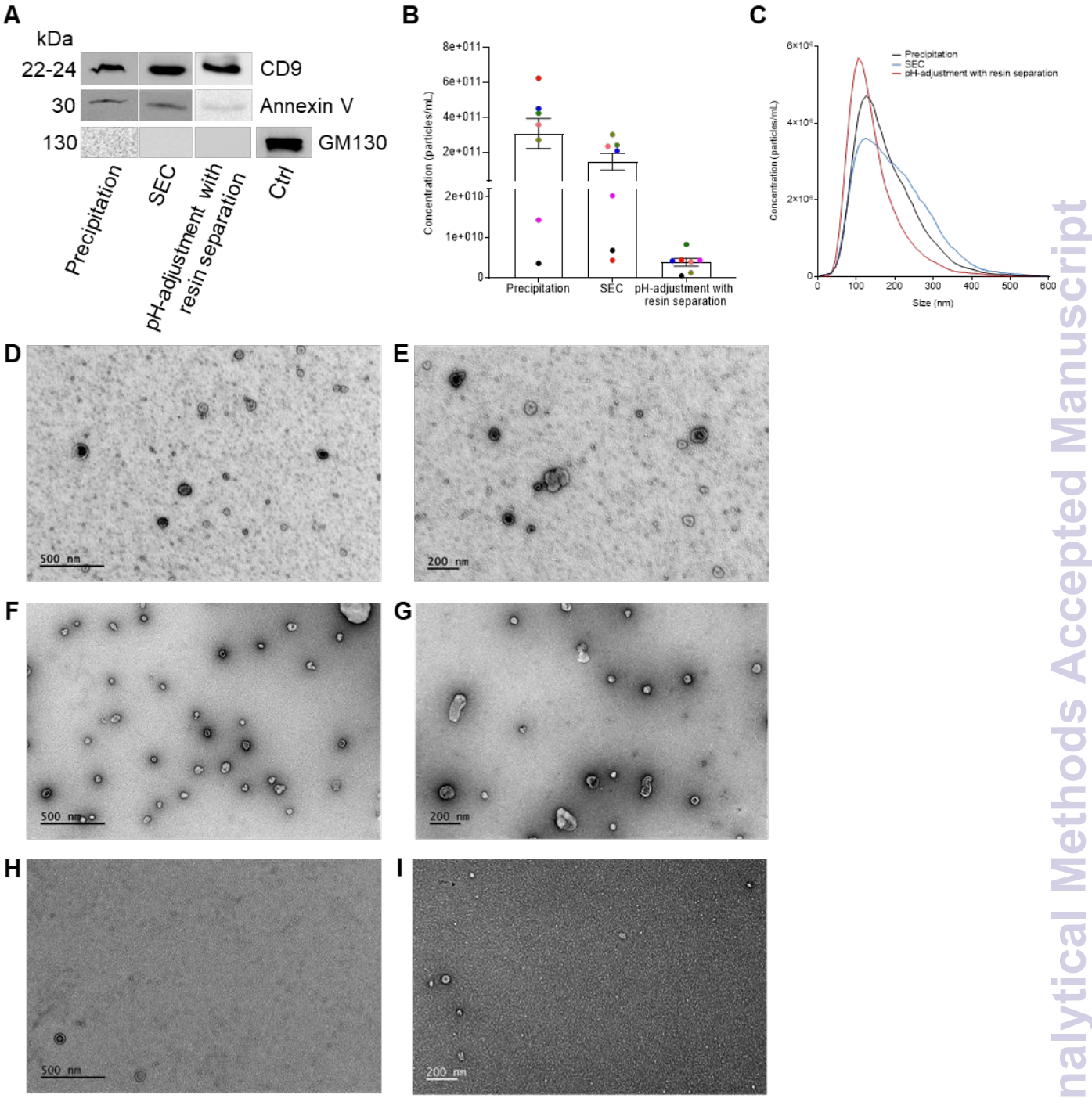

Fig 3. Characterisation of uEVs isolated by three different isolation methods. (A) uEV isolates were subjected to Western blotting analysis with antibodies specific for CD9, Annexin V and GM130. 'Ctrl' indicates positive control for GM130 (human foreskin fibroblast cell lysate). (B) Concentration and (C) size distribution of uEVs were measured by nanoparticle tracking analysis (NTA). (B) Data are presented as mean ± SEM and are from seven different human donors. (C) Data is the average of three technical replicates from one experiment with uEVs from one human

View Article Online
DOI: 10.1039/D6AY00002A

donor. (D-I) Representative images of negative stain transient electron microscopy (TEM) wide field (left - D, F, H) and close images (right – E, G, I) show uEV morphology. Scale bar 500 nm for wide field (D, F, H) and 200 nm for close images (E, G, I). (D,E) uEVs isolated by precipitation, (F, G) uEVs isolated by size exclusion chromatography, and (H, I) uEVs isolated by pH-adjustment with resin precipitation.

View Article Online
DOI: 10.1039/D6AY00002A

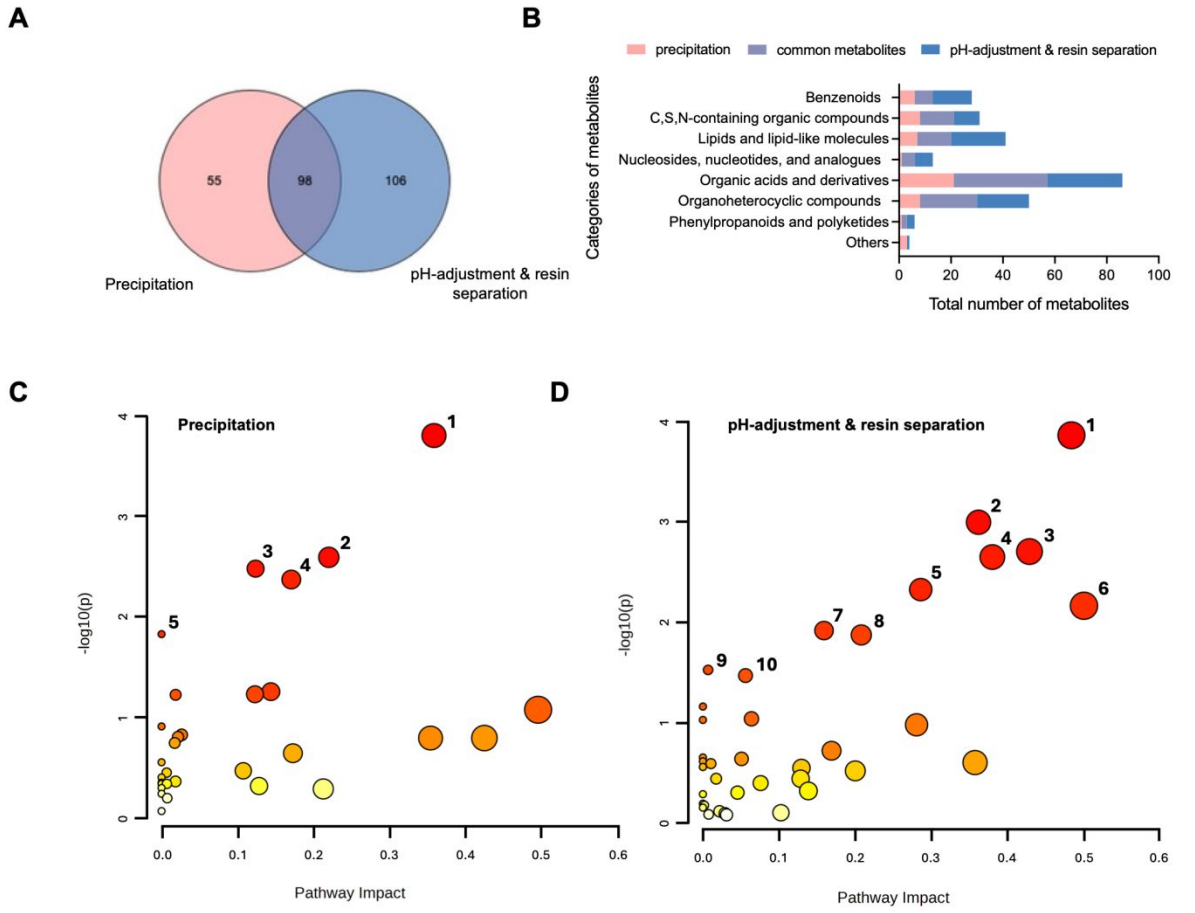

E

Precipitation

No.	Pathway Name	Number of Metabolites	*p*-value	FDR	Impact Score
1	Arginine biosynthesis	4	0.00014952	0.011962	0.3617
2	Alanine, aspartate and glutamate metabolism	4	0.0024724	0.082487	0.22195
3	Lysine degradation	4	0.0032104	0.082487	0.12474
4	Histidine metabolism	3	0.0041244	0.082487	0.17213
5	Ascorbate and aldarate metabolism	2	0.014513	0.23222	0.0

pH-adjustment & resin precipitation

No.	Pathway Name	Number of Metabolites	*p*-value	FDR	Impact Score
1	Histidine metabolism	5	0.00013396	0.010716	0.4836
2	Arginine biosynthesis	4	0.00098765	0.039506	0.3617
3	Taurine and hypotaurine metabolism	3	0.0019337	0.04387	0.42857
4	Alanine, aspartate and glutamate metabolism	5	0.0021935	0.04387	0.37981
5	Cysteine and methionine metabolism	5	0.0046421	0.074273	0.28585
6	Phenylalanine, tyrosine and tryptophan biosynthesis	2	0.0067266	0.089689	0.5
7	Tryptophan metabolism	5	0.011874	0.13129	0.15897
8	Tyrosine metabolism	5	0.013129	0.13129	0.20785
9	Pantothenate and CoA biosynthesis	3	0.02933	0.26071	0.0068
10	Beta-Alanine metabolism	3	0.033396	0.26717	0.05597

Fig 4. LC-MS analysis of metabolites extracted from uEVs obtained using different isolation methods. Comparison of metabolites identified by LC-MS that were extracted from uEVs isolated through precipitation-based and pH-adjustment and resin-separation methods. (A) Venn diagram displays number of metabolites shared and specific to uEVs isolated by

View Article Online
DOI: 10.1039/D6AY00002A

precipitation and pH-adjustment and resin-separation methods. (B) Number and categories of metabolites (based on the Human Metabolome Database) identified in uEVs isolated by precipitation and pH-adjustment and resin-separation methods. (C-D) Pathway analysis of identified metabolites that were extracted from uEVs isolated by precipitation (C) and pH adjustment and resin separation (D), respectively. Circles represent pathways with colour and size varying based on the p value and pathway impact value, respectively. Numbers represent the pathway name reported in (E). (E) Top 5 (top) and top 10 (bottom) significantly enriched pathways, with corresponding False Discovery Rate (FDR), p-value, and impact scores, obtained by metabolic pathway analysis of metabolites extracted from uEVs isolated by precipitation and pH adjustment and resin separation, respectively.[72]

View Article Online
DOI: 10.1039/D6AY00002A

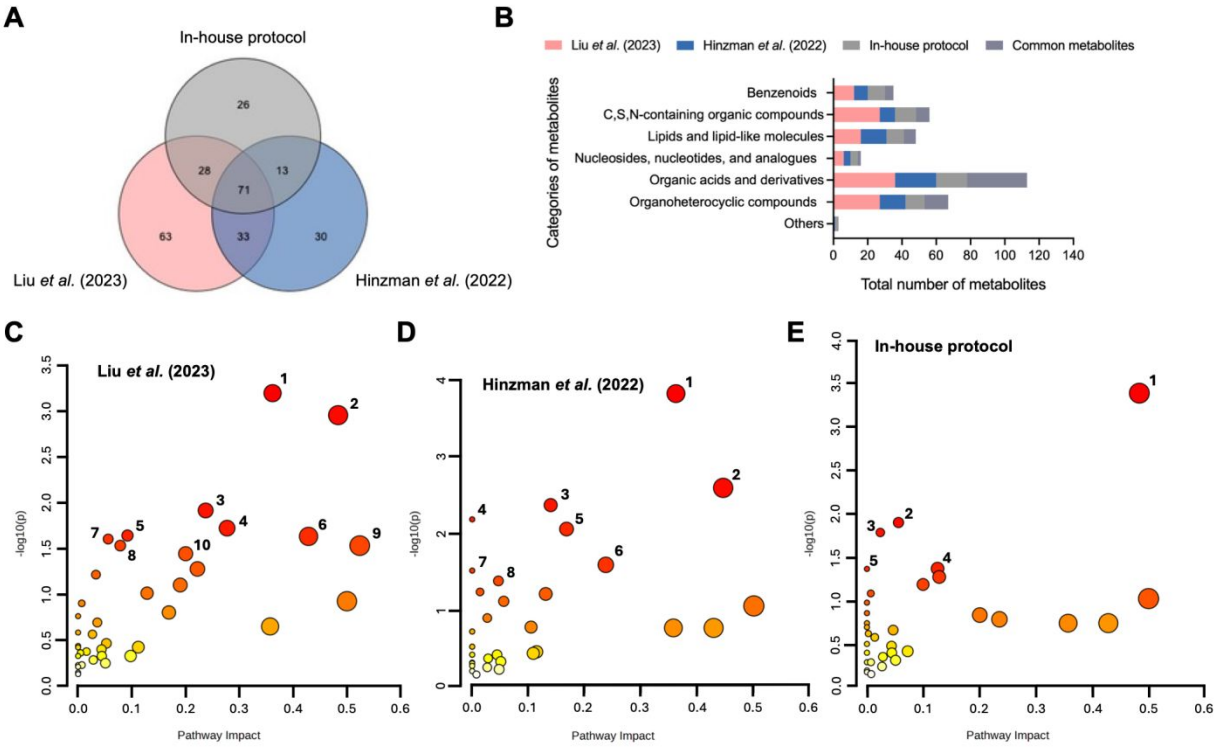

F

Liu *et al.*, 2023

No.	Pathway Name	Number of Metabolites	*p*-value	FDR	Impact Score
1	Arginine biosynthesis	4	0.00063272	0.043964	0.3617
2	Histidine metabolism	4	0.0010991	0.043964	0.4836
3	Lysine degradation	4	0.012042	0.25873	0.23721
4	Pentose and glucoronate interconversions	3	0.018772	0.25873	0.27711
5	Arginine and proline metabolism	4	0.022605	0.25873	0.09186
6	Taurine and hypotaurine metabolism	2	0.023088	0.25873	0.42857
7	Beta-Alanine metabolism	3	0.024678	0.25873	0.05597
8	Vitamin B6 metabolism	2	0.029107	0.25873	0.07843
9	Ascorbate and aldarate metabolism	2	0.029107	0.25873	0.52381
10	Biotin metabolism	2	0.035677	0.28542	0.2

Hinzman *et al.*, 2022

No.	Pathway Name	Number of Metabolites	*p*-value	FDR	Impact Score
1	Arginine biosynthesis	4	0.00014952	0.011962	0.3617
2	Alanine, aspartate and glutamate metabolism	4	0.0024724	0.098897	0.44552
3	Histidine metabolism	3	0.0041244	0.10998	0.13934
4	Nitrogen metabolism	2	0.0062958	0.12592	0.0
5	Pyrimidine metabolism	4	0.008407	0.13451	0.16747
6	Lysine degradation	3	0.02438	0.32506	0.23721
7	Glyoxylate and dicarboxylate metabolism	3	0.028932	0.33065	0.0
8	Arginine and proline metabolism	3	0.039304	0.39304	0.04651

In-house protocol

No.	Pathway Name	Number of Metabolites	*p*-value	FDR	Impact Score
1	Histidine metabolism	4	0.0004096	0.032768	0.4836
2	Beta-Alanine metabolism	3	0.012406	0.4299	0.05597
3	Tyrosine metabolism	4	0.016121	0.4299	0.02367
4	Cysteine and methionine metabolism	3	0.04181	0.6744	0.12535
5	Arginine metabolism	2	0.04215	0.6744	0.0

Fig 5. LC-MS analysis of metabolites extracted from uEVs using different extraction protocols. Comparison of the metabolites identified by LC-MS that were extracted from uEVs

View Article Online
DOI: 10.1039/D6AY00002A

using three different protocols: Liu *et al*. (2023), Hinzman *et al*. (2022), and the in-house developed protocol. uEVs were isolated by SEC. (A) Venn diagram displays number of metabolites shared and specific to each metabolite extraction protocol. (B) Number and categories of metabolites (based on the Human Metabolome Database) extracted from uEVs using different extraction protocols. (C) Pathway analysis of identified metabolites that were extracted from uEVs using the Liu *et al*., 2023 (C), Hinzman *et al*., 2022 (D), and in-house protocol (E), respectively. Circles represent pathways with colour and size varying based on the p value and pathway impact value, respectively. Numbers represent the pathway name reported in (F). (F) Top 10 (top), top 8 (middle) and top 5 (bottom) significantly enriched pathways, with corresponding False Discovery Rate (FDR), p-value, and impact scores, obtained by metabolic pathway analysis of metabolites extracted from uEVs, respectively using the Liu *et al*., 2023, Hinzman *et al*., 2022, and in-house protocol, respectively.

Author Contributions

CGA: Investigation, Formal analysis, Data curation, Methodology, Project administration, Validation, Visualization, Funding acquisition, Writing – original draft, Writing – review & editing. SMJ: Investigation, Formal analysis, Data curation, Methodology, Validation, Writing – original draft, Writing – review & editing. JKJR: Investigation, Writing – review & editing. GN: Investigation, Formal analysis, Writing – review & editing. KPA: Methodology, Writing – review & editing. VJ: Methodology, Writing – review & editing. MWT: Formal analysis, Methodology, Project administration, Supervision, Writing – review & editing. JJK: Conceptualization, Formal analysis, Methodology, Project administration, Supervision, Writing – review & editing. DHK: Formal analysis, Methodology, Validation, Visualization, Resources, Supervision, Writing – review & editing. AMP: Conceptualization, Data Curation, Formal analysis, Methodology, Validation, Visualization, Project administration, Resources, Supervision, Writing – original draft, Writing – review & editing. All authors reviewed and approved the final version of the manuscript.

View Article Online
DOI: 10.1039/D6AY00002A

Conflicts of Interest

The authors have no conflicts of interest to declare.

Data Availability

LC–MS metabolomics data for this article are available at Metabolomics Workbench repository (metabolomicsworkbench.org; Project PR002849) at http://dx.doi.org/10.21228/M8D84W. [73]

Funding

This work was supported by a PhD studentship to CGA from the Indonesia Endowment Fund for Education (LPDP), Ministry of Finance, Republic of Indonesia.

Acknowledgements

The authors would like to thank Alison Whitby (University of Nottingham) and Nathanael Ibot David, MD (Cipto Mangunkusumo Hospital, Central Jakarta, Indonesia) for assistance with metabolomics analysis. We also sincerely thank the Nanoscale and Microscale Research Centre, University of Nottingham, for providing access and support for the acquisition of TEM images.

Reference

1. Erdbrugger U, Blijdorp CJ, Bijnsdorp IV, Borras FE, Burger D, Bussolati B, et al. Urinary extracellular vesicles: a position paper by the urine task force of the international society for extracellular vesicles. J Extracell Vesicles. 2021;10(7):e12093. DOI: 10.1002/jev2.12093
2. Harpole M, Davis J, Espina V. Current state of the art for enhancing urine biomarker discovery. Expert Rev Proteomics. 2016;13(6):609–26. DOI: 10.1080/14789450.2016.1190651
3. Ambarsari CG, Tambunan T, Pardede SO, Fazlur Rahman FH, Kadaristiana A. Role of dipstick albuminuria in progression of paediatric chronic kidney disease. J Pak Med Assoc. 2021;71(Suppl 2)(2):S103–S6.
4. Ambarsari CG, Utami DAP, Tandri CC, Satari HI. Comparison of three spot proteinuria measurements for pediatric nephrotic syndrome: based on the International Pediatric Nephrology Association 2022 Guidelines. Ren Fail. 2023;45(2):2253324. DOI: 10.1080/0886022X.2023.2253324

View Article Online
DOI: 10.1039/D6AY00002A

5. Santiago-Rodriguez TM, Ly M, Bonilla N, Pride DT. The human urine virome in association with urinary tract infections. Front Microbiol. 2015;6:14. DOI: 10.3389/fmicb.2015.00014
6. Kalluri R, LeBleu VS. The biology, function, and biomedical applications of exosomes. Science. 2020;367(6478):eaau6977. DOI: 10.1126/science.aau6977
7. Chitti SV, Gummadi S, Kang T, Shahi S, Marzan AL, Nedeva C, et al. Vesiclepedia 2024: an extracellular vesicles and extracellular particles repository. Nucleic Acids Res. 2024;52(D1):D1694–D8. DOI: 10.1093/nar/gkad1007
8. Kang T, Atukorala I, Mathivanan S. Biogenesis of extracellular vesicles. Subcell Biochem. 2021;97:19–43. DOI: 10.1007/978-3-030-67171-6_2
9. Gyorgy B, Szabo TG, Pasztoi M, Pal Z, Misjak P, Aradi B, et al. Membrane vesicles, current state-of-the-art: emerging role of extracellular vesicles. Cell Mol Life Sci. 2011;68(16):2667–88. DOI: 10.1007/s00018-011-0689-3
10. Zhang H, Freitas D, Kim HS, Fabijanic K, Li Z, Chen H, et al. Identification of distinct nanoparticles and subsets of extracellular vesicles by asymmetric flow field-flow fractionation. Nat Cell Biol. 2018;20(3):332–43. DOI: 10.1038/s41556-018-0040-4
11. Di Bella MA. Overview and update on extracellular vesicles: considerations on exosomes and their application in modern medicine. Biology (Basel). 2022;11(6). DOI: 10.3390/biology11060804
12. Couch Y, Buzas EI, Di Vizio D, Gho YS, Harrison P, Hill AF, et al. A brief history of nearly EV-erything - the rise and rise of extracellular vesicles. J Extracell Vesicles. 2021;10(14):e12144. DOI: 10.1002/jev2.12144
13. Sun IO, Lerman LO. Urinary extracellular vesicles as biomarkers of kidney disease: from diagnostics to therapeutics. Diagnostics (Basel). 2020;10(5):311. DOI: 10.3390/diagnostics10050311
14. Roy S, Hochberg FH, Jones PS. Extracellular vesicles: the growth as diagnostics and therapeutics; a survey. J Extracell Vesicles. 2018;7(1):1438720. DOI: 10.1080/20013078.2018.1438720
15. Logozzi M, Angelini DF, Giuliani A, Mizzoni D, Di Raimo R, Maggi M, et al. Increased plasmatic levels of PSA-expressing exosomes distinguish prostate cancer patients from benign prostatic hyperplasia: a prospective study. Cancers (Basel). 2019;11(10):1449. DOI: 10.3390/cancers11101449
16. Zhai LY, Li MX, Pan WL, Chen Y, Li MM, Pang JX, et al. In situ detection of plasma exosomal microRNA-1246 for breast cancer diagnostics by a Au nanoflare probe. ACS Appl Mater Interfaces. 2018;10(46):39478–86. DOI: 10.1021/acsami.8b12725
17. Xylaki M, Chopra A, Weber S, Bartl M, Outeiro TF, Mollenhauer B. Extracellular vesicles for the diagnosis of Parkinson's disease: systematic review and meta-analysis. Mov Disord. 2023;38(9):1585–97. DOI: 10.1002/mds.29497
18. Karpman D, Stahl AL, Arvidsson I. Extracellular vesicles in renal disease. Nat Rev Nephrol. 2017;13(9):545–62. DOI: 10.1038/nrneph.2017.98
19. Merchant ML, Rood IM, Deegens JKJ, Klein JB. Isolation and characterization of urinary extracellular vesicles: implications for biomarker discovery. Nat Rev Nephrol. 2017;13(12):731–49. DOI: 10.1038/nrneph.2017.148
20. Tutrone R, Lowentritt B, Neuman B, Donovan MJ, Hallmark E, Cole TJ, et al. ExoDx prostate test as a predictor of outcomes of high-grade prostate cancer - an interim analysis. Prostate Cancer Prostatic Dis. 2023;26(3):596–601. DOI: 10.1038/s41391-023-00675-1
21. Tutrone R, Donovan MJ, Torkler P, Tadigotla V, McLain T, Noerholm M, et al. Clinical utility of the exosome based ExoDx Prostate (IntelliScore) EPI test in men presenting for initial biopsy with a PSA 2-10 ng/mL. Prostate Cancer Prostatic Dis. 2020;23(4):607–14. DOI: 10.1038/s41391-020-0237-z

View Article Online
DOI: 10.1039/D6AY00002A

22. Exosome Diagnostics. FDA grants breakthrough device designation to Bio-Techne's ExoDx Prostate (IntelliScore) (EPI) Test 2019 [cited 2024 July 10]. Available from: https://www.exosomedx.com/news-events/fda-grants-breakthrough-device-designation-bio-technes-exodx-prostate-intelliscore-epi.
23. Thery C, Witwer KW, Aikawa E, Alcaraz MJ, Anderson JD, Andriantsitohaina R, et al. Minimal information for studies of extracellular vesicles 2018 (MISEV2018): a position statement of the International Society for Extracellular Vesicles and update of the MISEV2014 guidelines. J Extracell Vesicles. 2018;7(1):1535750. DOI: 10.1080/20013078.2018.1535750
24. Park S, Lee K, Park IB, Kim NH, Cho S, Rhee WJ, et al. The profiles of microRNAs from urinary extracellular vesicles (EVs) prepared by various isolation methods and their correlation with serum EV microRNAs. Diabetes Res Clin Pract. 2020;160:108010. DOI: 10.1016/j.diabres.2020.108010
25. Bokhove M, Nishimura K, Brunati M, Han L, de Sanctis D, Rampoldi L, et al. A structured interdomain linker directs self-polymerization of human uromodulin. Proc Natl Acad Sci U S A. 2016;113(6):1552–7. DOI: 10.1073/pnas.1519803113
26. Dudzik D, Macioszek S, Struck-Lewicka W, Kordalewska M, Buszewska-Forajta M, Waszczuk-Jankowska M. Perspectives and challenges in extracellular vesicles untargeted metabolomics analysis. Trends Analyt Chem. 2021;143:116382. DOI: 10.1016/j.trac.2021.116382
27. Luo P, Mao K, Xu J, Wu F, Wang X, Wang S, et al. Metabolic characteristics of large and small extracellular vesicles from pleural effusion reveal biomarker candidates for the diagnosis of tuberculosis and malignancy. J Extracell Vesicles. 2020;9(1):1790158. DOI: 10.1080/20013078.2020.1790158
28. Want EJ, O'Maille G, Smith CA, Brandon TR, Uritboonthai W, Qin C, et al. Solvent-dependent metabolite distribution, clustering, and protein extraction for serum profiling with mass spectrometry. Anal Chem. 2006;78(3):743–52. DOI: 10.1021/ac051312t
29. Sostare J, Di Guida R, Kirwan J, Chalal K, Palmer E, Dunn WB, et al. Comparison of modified Matyash method to conventional solvent systems for polar metabolite and lipid extractions. Anal Chim Acta. 2018;1037:301–15. DOI: 10.1016/j.aca.2018.03.019
30. Correa R, Coronado LM, Garrido AC, Durant-Archibold AA, Spadafora C. Volatile organic compounds associated with *Plasmodium falciparum* infection in vitro. Parasit Vectors. 2017;10(1):215. DOI: 10.1186/s13071-017-2157-x
31. Stam J, Bartel S, Bischoff R, Wolters JC. Isolation of extracellular vesicles with combined enrichment methods. J Chromatogr B Analyt Technol Biomed Life Sci. 2021;1169:122604. DOI: 10.1016/j.jchromb.2021.122604
32. Life Technologies Corporation. Total exosome isolation from urine 2013 [cited 2024 July 10]. Available from: https://www.thermofisher.com/document-connect/document-connect.html?url=https%3A%2F%2Fassets.thermofisher.com%2FTFS-Assets%2FLSG%2Fmanuals%2Ftotal_exosome_urine_man.pdf.
33. IZON Science. qEV series comparison 2025 [cited 2025 March 14]. Available from: https://www.izon.com/qev/qev-series-comparison.
34. IZON Science. qEVsingle Gen 2 user manual 2025 [cited 2025 March 24]. Available from: https://4136435.fs1.hubspotusercontent-na1.net/hubfs/4136435/Manuals%20Technical%20Notes%20and%20Customer%20Support/qEV%20columns/qEVsingle-gen-2-user-manual-ICS-DQ-001.pdf
35. IZON Science. qEVsingle concentration kit user manual 2020 [cited 2024 July 10]. Available from: https://files.izon.com/hubfs/Manuals%20Technical%20Notes%20and%20Customer%20Support/qEV%20Concentration%20Kit/qEV%20concentration%20kit%20user%20manual.pdf

View Article Online
DOI: 10.1039/D6AY00002A

36. Norgen Biotek Corporation. Urine exosome purification kits product insert 2015 [cited 2024 July 10]. Available from: https://norgenbiotek.com/sites/default/files/resources/Urine-Exosome-Purification-Kits-Insert-PI57700-2.pdf.
37. System Biosciences. ExoGlow-NTA™ fluorescent labeling kit (for Particle Metrix ZetaView®) 2022 [cited 2024 July 10]. Available from: https://www.systembio.com/wp/wp-content/uploads/2020/10/MANUAL_ExoGlow-NTA-PMX_V4.pdf.
38. Auger C, Brunel A, Darbas T, Akil H, Perraud A, Begaud G, et al. Extracellular vesicle measurements with nanoparticle tracking analysis: a different appreciation of up and down secretion. Int J Mol Sci. 2022;23(4):2310. DOI: 10.3390/ijms23042310
39. Bachurski D, Schuldner M, Nguyen PH, Malz A, Reiners KS, Grenzi PC, et al. Extracellular vesicle measurements with nanoparticle tracking analysis - an accuracy and repeatability comparison between NanoSight NS300 and ZetaView. J Extracell Vesicles. 2019;8(1):1596016. DOI: 10.1080/20013078.2019.1596016
40. Liu P, Wang W, Wang F, Fan J, Guo J, Wu T, et al. Alterations of plasma exosomal proteins and motabolies are associated with the progression of castration-resistant prostate cancer. J Transl Med. 2023;21(1):40. DOI: 10.1186/s12967-022-03860-3
41. Hinzman CP, Jayatilake M, Bansal S, Fish BL, Li Y, Zhang Y, et al. An optimized method for the isolation of urinary extracellular vesicles for molecular phenotyping: detection of biomarkers for radiation exposure. J Transl Med. 2022;20(1):199. DOI: 10.1186/s12967-022-03414-7
42. Clos-Sansalvador M, Monguio-Tortajada M, Roura S, Franquesa M, Borras FE. Commonly used methods for extracellular vesicles' enrichment: implications in downstream analyses and use. Eur J Cell Biol. 2022;101(3):151227. DOI: 10.1016/j.ejcb.2022.151227
43. Reseco L, Molina-Crespo A, Atienza M, Gonzalez E, Falcon-Perez JM, Cantero JL. Characterization of extracellular vesicles from human saliva: effects of age and isolation techniques. Cells. 2024;13(1):95. DOI: 10.3390/cells13010095
44. Shirejini SZ, Inci F. The Yin and Yang of exosome isolation methods: conventional practice, microfluidics, and commercial kits. Biotechnol Adv. 2022;54:107814. DOI: 10.1016/j.biotechadv.2021.107814
45. Macias M, Rebmann V, Mateos B, Varo N, Perez-Gracia JL, Alegre E, et al. Comparison of six commercial serum exosome isolation methods suitable for clinical laboratories. Effect in cytokine analysis. Clin Chem Lab Med. 2019;57(10):1539–45. DOI: 10.1515/cclm-2018-1297
46. Veerman RE, Teeuwen L, Czarnewski P, Gucluler Akpinar G, Sandberg A, Cao X, et al. Molecular evaluation of five different isolation methods for extracellular vesicles reveals different clinical applicability and subcellular origin. J Extracell Vesicles. 2021;10(9):e12128. DOI: 10.1002/jev2.12128
47. Sidhom K, Obi PO, Saleem A. A review of exosomal isolation methods: is size exclusion chromatography the best option? Int J Mol Sci. 2020;21(18):6466. DOI: 10.3390/ijms21186466
48. Jia Y, Yu L, Ma T, Xu W, Qian H, Sun Y, et al. Small extracellular vesicles isolation and separation: current techniques, pending questions and clinical applications. Theranostics. 2022;12(15):6548–75. DOI: 10.7150/thno.74305
49. Arntz OJ, Pieters BCH, van Lent P, Koenders MI, van der Kraan PM, van de Loo FAJ. An optimized method for plasma extracellular vesicles isolation to exclude the copresence of biological drugs and plasma proteins which impairs their biological characterization. Plos One. 2020;15(7):e0236508. DOI: 10.1371/journal.pone.0236508
50. Konoshenko MY, Lekchnov EA, Vlassov AV, Laktionov PP. Isolation of extracellular vesicles: general methodologies and latest trends. Biomed Res Int. 2018;2018:8545347. DOI: 10.1155/2018/8545347

View Article Online
DOI: 10.1039/D6AY00002A

51. Vychytilova-Faltejskova P, Vilmanova S, Pifkova L, Catela Ivkovic T, Mądrzyk M, Jugas R, et al. Optimized procedure for high-throughput transcriptome profiling of small extracellular vesicles isolated from low volume serum samples. Clin Chem Lab Med. 2024;62(1):157–67. DOI: 10.1515/cclm-2023-0610
52. Land KJ, Boeras DI, Chen XS, Ramsay AR, Peeling RW. REASSURED diagnostics to inform disease control strategies, strengthen health systems and improve patient outcomes. Nat Microbiol. 2019;4(1):46–54. DOI: 10.1038/s41564-018-0295-3
53. Larkins MC, Thombare A. Point-of-care testing. StatPearls. Treasure Island (FL)2025.
54. Palupi-Baroto R, Hermawan K, Murni IK, Nurlita T, Prihastuti Y, Puspitawati I, et al. Carotid intima-media thickness, fibroblast growth factor 23, and mineral bone disorder in children with chronic kidney disease. Bmc Nephrol. 2024;25(1):369. DOI: 10.1186/s12882-024-03771-z
55. Savva KV, Kawka M, Vadhwana B, Penumaka R, Patton I, Khan K, et al. The biomarker toolkit - an evidence-based guideline to predict cancer biomarker success and guide development. Bmc Med. 2023;21(1):383. DOI: 10.1186/s12916-023-03075-3
56. Schrimpe-Rutledge AC, Codreanu SG, Sherrod SD, McLean JA. Untargeted metabolomics strategies-challenges and emerging directions. J Am Soc Mass Spectrom. 2016;27(12):1897–905. DOI: 10.1007/s13361-016-1469-y
57. Palviainen M, Saari H, Karkkainen O, Pekkinen J, Auriola S, Yliperttula M, et al. Metabolic signature of extracellular vesicles depends on the cell culture conditions. J Extracell Vesicles. 2019;8(1):1596669. DOI: 10.1080/20013078.2019.1596669
58. Williams C, Palviainen M, Reichardt NC, Siljander PR, Falcon-Perez JM. Metabolomics applied to the study of extracellular vesicles. Metabolites. 2019;9(11). DOI: 10.3390/metabo9110276
59. Ivanisevic J, Zhu ZJ, Plate L, Tautenhahn R, Chen S, O'Brien PJ, et al. Toward 'omic scale metabolite profiling: a dual separation-mass spectrometry approach for coverage of lipid and central carbon metabolism. Anal Chem. 2013;85(14):6876–84. DOI: 10.1021/ac401140h
60. Shin MH, Lee DY, Liu KH, Fiehn O, Kim KH. Evaluation of sampling and extraction methodologies for the global metabolic profiling of Saccharophagus degradans. Anal Chem. 2010;82(15):6660–6. DOI: 10.1021/ac1012656
61. Puhka M, Takatalo M, Nordberg ME, Valkonen S, Nandania J, Aatonen M, et al. Metabolomic profiling of extracellular vesicles and alternative normalization methods reveal enriched metabolites and strategies to study prostate cancer-related changes. Theranostics. 2017;7(16):3824–41. DOI: 10.7150/thno.19890
62. Zang X, Monge ME, Fernandez FM. Mass spectrometry-based non-targeted metabolic profiling for disease detection: recent developments. Trends Analyt Chem. 2019;118:158–69. DOI: 10.1016/j.trac.2019.05.030
63. Ranjha MMAN, Irfan S, Lorenzo JM, Shafique B, Kanwal R, Pateiro M, et al. Sonication, a potential technique for extraction of phytoconstituents: a systematic review. Processes. 2021;9(8):1406. DOI: 10.3390/pr9081406
64. Le Saux S, Aarrass H, Lai-Kee-Him J, Bron P, Armengaud J, Miotello G, et al. Post-production modifications of murine mesenchymal stem cell (mMSC) derived extracellular vesicles (EVs) and impact on their cellular interaction. Biomaterials. 2020;231:119675. DOI: 10.1016/j.biomaterials.2019.119675
65. Chen Y, Wang L, Yu X, Mao W, Wan Y. Ultrasonication outperforms electroporation for extracellular vesicle cargo depletion. Extracell Vesicle. 2024;4. DOI: 10.1016/j.vesic.2024.100052
66. Lee JE, Jayakody JTM, Kim JI, Jeong JW, Choi KM, Kim TS, et al. The influence of solvent choice on the extraction of bioactive compounds from Asteraceae: a comparative review. Foods. 2024;13(19):3151. DOI: 10.3390/foods13193151

View Article Online
DOI: 10.1039/D6AY00002A

67. Amaro HM, Fernandes F, Valentao P, Andrade PB, Sousa-Pinto I, Malcata FX, et al. Effect of solvent system on extractability of lipidic components of *Scenedesmus obliquus* (M2-1) and *Gloeothece sp.* on antioxidant scavenging capacity thereof. Mar Drugs. 2015;13(10):6453–71. DOI: 10.3390/md13106453
68. Nguyen MHL, DiPasquale M, Rickeard BW, Stanley CB, Kelley EG, Marquardt D. Methanol accelerates DMPC flip-flop and aransfer: a SANS study on lipid dynamics. Biophys J. 2019;116(5):755–9. DOI: 10.1016/j.bpj.2019.01.021
69. Saini RK, Prasad P, Shang X, Keum Y-S. Advances in lipid extraction methods—a review. Int J Mol Sci. 2021;22(24):13643. DOI: 10.3390/ijms222413643
70. Maia M, Monteiro F, Sebastiana M, Marques AP, Ferreira AEN, Freire AP, et al. Metabolite extraction for high-throughput FTICR-MS-based metabolomics of grapevine leaves. EuPA Open Proteomics. 2016;12:4–9. DOI: 10.1016/j.euprot.2016.03.002
71. Yoshida K, Mitsumori R, Horii K, Takashima A, Nishio I. Acetonitrile-induced destabilization in liposomes. Colloids Interfaces. 2018;2(1):6. DOI: 10.3390/colloids2010006
72. Xia J, Mandal R, Sinelnikov IV, Broadhurst D, Wishart DS. MetaboAnalyst 2.0--a comprehensive server for metabolomic data analysis. Nucleic Acids Res. 2012;40(Web Server issue):W127–33. DOI: 10.1093/nar/gks374
73. Sud M, Fahy E, Cotter D, Azam K, Vadivelu I, Burant C, et al. Metabolomics Workbench: An international repository for metabolomics data and metadata, metabolite standards, protocols, tutorials and training, and analysis tools. Nucleic Acids Res. 2016;44(D1):D463–70. DOI: 10.1093/nar/gkv1042

Data Availability

LC–MS metabolomics data for this article are available at Metabolomics Workbench repository (metabolomicsworkbench.org; Project PR002849) at http://dx.doi.org/10.21228/M8D84W. [73]